ORIGINAL RESEARCH

Carbon fiber/epoxy resin/α-aluminum oxide nanocomposites; fabrication, mechanical and thermal analysis

Hossein Chamkouri[1] · Malihe Pooresmaeil[1] · Hassan Namazi[1]

Abstract

A composite is a material having two or more components with diverse chemical or physical properties. Due to the special feature of the composites, the use of various materials and research in their field is developing. By considering the above points, in this work a series of the nanocomposites from α-Al$_2$O$_3$ nanoparticles (α-Al$_2$O$_3$ NPs, at 2, 5, and 10% by wt), carbon fibers (CF), and epoxy resin were fabricated and their thermal and mechanical performance were evaluated. The dispersion mode of α-Al$_2$O$_3$ NPs in the composite structure was evaluated through a field emission scanning electron microscope (FE-SEM). The FE-SEM analysis revealed that the α-Al$_2$O$_3$ NPs and CF were homogeneously dispersed in the epoxy matrix and the morphology of α-Al$_2$O$_3$ NPs–CF/epoxy composites is uniform. The results of the mechanical tests exhibited that the flexural strength and module of E-40 (epoxy resin: carbon fiber: α-Al$_2$O$_3$, 65:25:10) were at their highest levels; 295 MPa and 11,917 MPa, respectively. For flexural strength and module, improvements were made by 95.5% and 91.8% in comparison with the samples in the absence of NPs. The highest tensile strength was obtained for E-30 (epoxy resin: carbon fiber: α-Al$_2$O$_3$, 70:25:5); 341 MPa. There is a 24% enhancement in tensile strength as compression by a sample without NPs. Accordingly, we can conclude that the addition of α-Al$_2$O$_3$ NPs in composite structures has significantly affected the mechanical response. However, the thermal analysis was illustrated as an inverse trend by the addition of NPs. Therefore, the performance of experimental tests revealed that the composite with the required feature could be prepared based on the obtained results.

Keywords α-Al$_2$O$_3$ Nanoparticles · Epoxy resin · Carbon fiber · Composite properties · Mechanical strength

Introduction

Researchers need to reduce the weight of new structures as much as possible to prevent aircraft from falling. Ever since men first experienced flying, they have always tried to reduce the ratio of thrust to weight in aircrafts to avoid the risk of falling. In recent years, composites play an important role in reducing the weight of aircraft. Epoxy resin composite and carbon, glass, and aramid fibers are some of these composites. Composites are so efficient that they can be used in both structural components and parts of aircraft and spacecraft. From hot air balloons and drones to passenger planes and fighter jets and space shuttles, everyone benefits from composites [1–3].

Today, the NPs- and CF-reinforced polymer (CFRP) composites are progressively replacing the high-density and thick metal components because of their high specific strength, high durability, and low density [4–6]. A composite is a material which contains the matrix and one or more fillers [7–9]. Therefore, these materials display the benefit of both portions [10–12]. More study on the published works reveal that various NPs have been used as a nanoportion of nanocomposites [13–15]. In addition, a composite could be proposed as the best candidate for various applications [16–18]. Composites having CF reinforcement have a higher mechanical strength in comparison with other fibers such as glass fiber. However, the CF-reinforced polymer composites are much more expensive than glass fiber-reinforced polymer (GFRP) composites [19–21]. The optimized features like price and mechanical performance can be accomplished through the hybridization of NPs and CF [22–24].

✉ Hassan Namazi
  namazi@tabrizu.ac.ir

1   Research Laboratory of Dendrimers and Natural Polymers, Faculty of Chemistry, University of Tabriz, P.O. Box: 5166616471, Tabriz, Iran

Alternatively, inorganic nanofillers with low prices, for example, Al_2O_3 NPs could be added to CF-reinforced polymer composites to enhance their interlaminar shear strength and flexural properties [25–27]. The metal oxides (Al, Fe, etc.), carbonaceous-based particles (graphene, multi-walled carbon nanotubes (MWCNTs), single-wall carbon nanotubes (SWCNTs), etc.), inorganic particles (SiC, SiO_2, etc.), and other supplies (nanoclay, WS_2, MoS_2, etc.)) can increase the mechanical performance of composite structures [28–30]. Between countless metal or inorganic-based nanostructure, Al_2O_3 NPs is a uniquely recognized nanostructure because of its superior mechanical properties and the low price in manufacturing procedure in comparison with the carbonaceous nanomaterial [31–33]. The polymeric hybrid composites are extensively preferred and accepted because of the extraordinary strength of carbon fiber, as well as, due to the valuable balancing properties of hybridization [34–36]. The theoretical study has shown that hybridization influences the outcomes due to changes in carbon fiber modulus that balances the properties of polymeric hybrid composites [37–39]. Long-lasting CFRP composites are proposed as one of the main components in automotive industry applications because they have light-weight and easy processing. Although their mechanical strength and stiffness should be enhanced for use in the numerous mechanical components. To enhance these features, reinforcing agents are frequently used [36, 40, 41]. When stiff fillers are utilized to raise rigidity, the bending aspect of polymer matrices provides enormous toughness. In this way, the interfacial bond between the matrix, filler, and CF is a requirement for effectual load distribution and acceptable mechanical properties. Therefore, in the last decades, the main research has focused on how to develop the interfacial relationship between components for attaining the anticipated mechanical properties [42–44].

The literature assessments display that there is a restricted quantity of research works that emphasizes the influence of α-Al_2O_3 NPs loading into CF/epoxy hybrid composites. Depending on these investigations, it is vital to examine the influence of α-Al_2O_3 NPs adaptation on CF strengthened epoxy composite systems. Therefore, by considering the above-cited points, in the present study, two types of polymeric composites, CF/epoxy resin and α-Al_2O_3/CF/epoxy resin, were prepared. In the following, the effect of α-Al_2O_3 NPs (0, 2, 5, and 10% by wt) on the void content (%) and thermal behavior of the CF-reinforced composite samples was investigated. Compared to the previously published research works, in this research paper, using acetone led to the proper distribution and dispersion of α-Al_2O_3 NPs at different amounts. This factor gave rise to appropriate mechanical behavior of the composite structure modified with α-Al_2O_3 NPs. Also, the modified composite structure in this work displayed a better ability to absorb stresses and

prevent the growth of cracks in small dimensions in comparison with other works [40, 45, 46]. In the following, the mechanical properties of CF/epoxy are evaluated. Additionally, feasible structural interaction has been investigated for the monitoring of surface fracture and its failure using FE-SEM analysis.

Experimental

Materials

The woven carbon fiber was utilized as fiber strengthening in the hybrid composite structure. The CF was a product from Xiamen LFT Composite Plastic Company, China. The epoxy (polymer) resin of Bisphenol-A as a matrix phase and triethylene tetramine (TETA) as a curing agent was purchased from Bite Company, The Netherlands; and α-Al_2O_3 NPs with an average diameter of about 90 nm were purchased from the US-Nano Company, USA.

Composite fabrication

The NPs distribution into the polymeric resin plays an important effect on the mechanical properties of the polymeric composites. In this regard, firstly the α-Al_2O_3 NPs (2, 5, and 10% by wt) were distributed into acetone by sonication for 10 min to obtain a fully dispersed NPs dispersion [31]. In the following, the obtained suspension was merged with the epoxy resin. The epoxy resin was then added to the NPs suspension, and the mixture was subjected to ultrasonic friction for 30 min. A total of 40 min were the ultrasonic process time [3]. Afterward, acetone was eliminated from the resin structure by keeping it in a vacuum oven (80 °C for 20 h). The uniform dispersion of NPs in the composite structure is revealed in FE-SEM images. As a final point, the curing agent, as a hardener, merged into the mixture of resin and NPs through provider orders (physically mixed for 10 min). The epoxy resin reacts with the hardener to form cross-links between the chains, and the resin changes phase from liquid to solid. The unmodified epoxy structure was similarly organized at identical conditions for controlling the accuracy of experimental investigation. The schematic illustration of the procedure is shown in Fig. 1. CF strengthened modified polymeric composite structures were fabricated through the hand layup technique. The compositions of the hybrid composites are reported in Table 1. In the hand layup technique, before placing the fibers into the metal mold, we impregnated it with epoxy resin modified by NPs. Then, 5 layers of carbon fiber were inserted into the mold, and pressure was applied to the samples using a manual tap, which led to the release of trapped air inside the layers. Subsequently, the temperature was adjusted at 90 °C for 45 min and 130 °C for
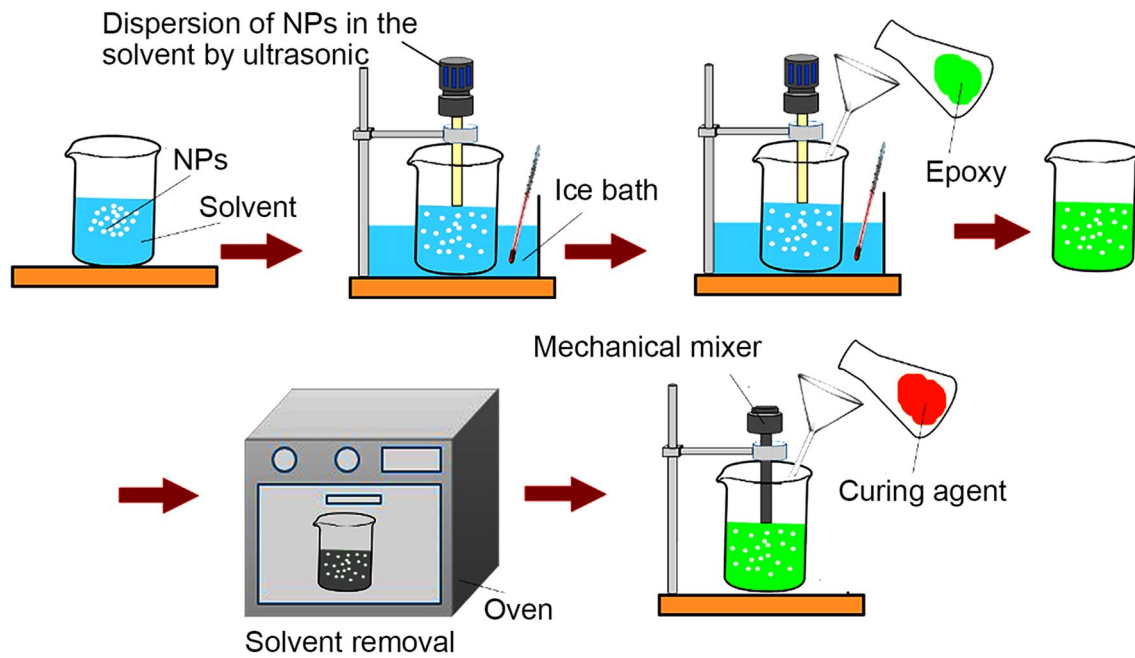
Fig. 1 Schematic presentation of the epoxy resin matrix modification

Table 1 The amount of epoxy resin, CF, and α-Al$_2$O$_3$ NPs (expressed in % by wt) for the preparation of hybrid composites

Classification of samples	Sample	Epoxy resin by wt))%	Carbon fiber % (by wt)	α-Al$_2$O$_3$ % (by wt)
Prototype sample	E-10	75	25	–
	E-20	73	25	2
Advance samples	E-30	70	25	5
	E-40	65	25	10

1 h. The hybrid composite structures were exposed to switch cooling while waiting for lowering of ambient temperature to stop the unexpected shrinkage. The compositions of the hybrid composites are reported in Table 1.

Void content investigation

In the procedure of hand lay-up fabrication, the creation of the void in the structure is non-preventable. On the other hand, poorer void content has a positive effect on raising the reliability and durability of the hybrid composites. In this work, the void contents of the composites were calculated through Eq. 1. In Eq. 1, the ρ_t is the theoretic composite density, and ρ_e is the calculated density of samples.

$$V(\%) = \frac{\rho_t - \rho_e}{\rho_t} \times 100 \tag{1}$$

The following equation shows how the theoretical density can be calculated:

$$\rho t = \frac{1}{\frac{W_{CF}}{\rho_{CF}} + \frac{W_{NPs}}{\rho_{NPs}} + \frac{W_{resin}}{\rho_{re\,sin}}} \tag{2}$$

where W_{CF}, W_{NPs}, and W_{resin} are the carbon fiber, NPs, resin weight fractions, while ρ_{resin}, $\rho_{carbon\,fiber}$, and ρ_{NPs} are the densities of the resin, carbon fiber, and NPs.

Mechanical study

After composite fabrication, the samples were subjected to mechanical tests to determine their mechanical properties such as tensile strength using a Universal Testing Machine. The tensile test was done through the ZTM20 model. The applied loading rate was 1 mm/min. The flexural testing machine was used to obtain the highest mechanical resistance in bending. The flexural test was done by ASTM D 790 standard. The test speed was adjusted at 1 mm/min [47]. A 3-point bending was carried out by the ZTM20 model. These two tests illustrate the sample behavior in bending. Moreover, the thickness of each layer of the structure is 0.304 mm. Besides, hardness is recognized as the resistance toward perpetual indentation. This assessment measures plastic deformation resistance in the layers of hybrid composite structures. Brinell hardness assessment was operated on the sample by a Brinell machine. The hardness test was examined at four different samples with α-Al$_2$O$_3$ NPs

(0, 2, 5, and 10% by wt). The hardness and indentation were calculated and measured by Eq. 3.

$$BNH = \frac{2F}{\pi D\left(D - \sqrt{D^2 - d^2}\right)} \tag{3}$$

where: F = applied load in N; D = diameter of the indenter; d = diameter of impression.

Morphology analysis

A field emission scanning electron microscope (FE-SEM) was used to study the dispersion mode of α-Al_2O_3 NPs in the composite structure. The morphology of the samples such as fracture behavior, fiber-matrix interaction, and fiber pull-out, after undergoing the mechanical tests was investigated using MIRA 3 Tescan FE-SEM. The samples were coated with gold before FE-SEM analysis. Imaging was carried out at 15 kV.

Thermal analysis

The effect of α-Al_2O_3 NPs on the thermal properties of carbon fiber/epoxy resin hybrid composites was studied using thermogravimetric analysis (TGA). Samples were heated in the temperature range of 30 °C–750 °C under a controlled nitrogen atmosphere with a heating rate of 20 °C/min. The

obtained data from the TGA analysis were used to determine the thermal stability of the samples.

Results and discussion

Void content

Figure 2 displays the void content (%) of the fabricated composites versus the types of composite samples. It is detected that the void content of composites of samples E-10, E-20, E30, and E-40 is 1.2%, 1.6%, 1.5%, and 1.5%, respectively. The fabricated composite structures of different layers have different percentages of voids and the presence of additives. Nevertheless, because of superior adhesiveness and wettability of epoxy resin with carbon fiber and other additives, the presence of voids is lowest in the CFRP composites without any Al_2O_3 NPs.

Mechanical investigation

With the purpose of conducting a mechanical performance, we measured the most accurate values and the standard deviation of the samples such as the tensile strength, the flexural strength, and the flexural modulus (Fig. 3). For evaluation of the mechanical behaviors, each sample was tested three-times and the average results were reported

Fig. 2 Void content of the prepared composite samples
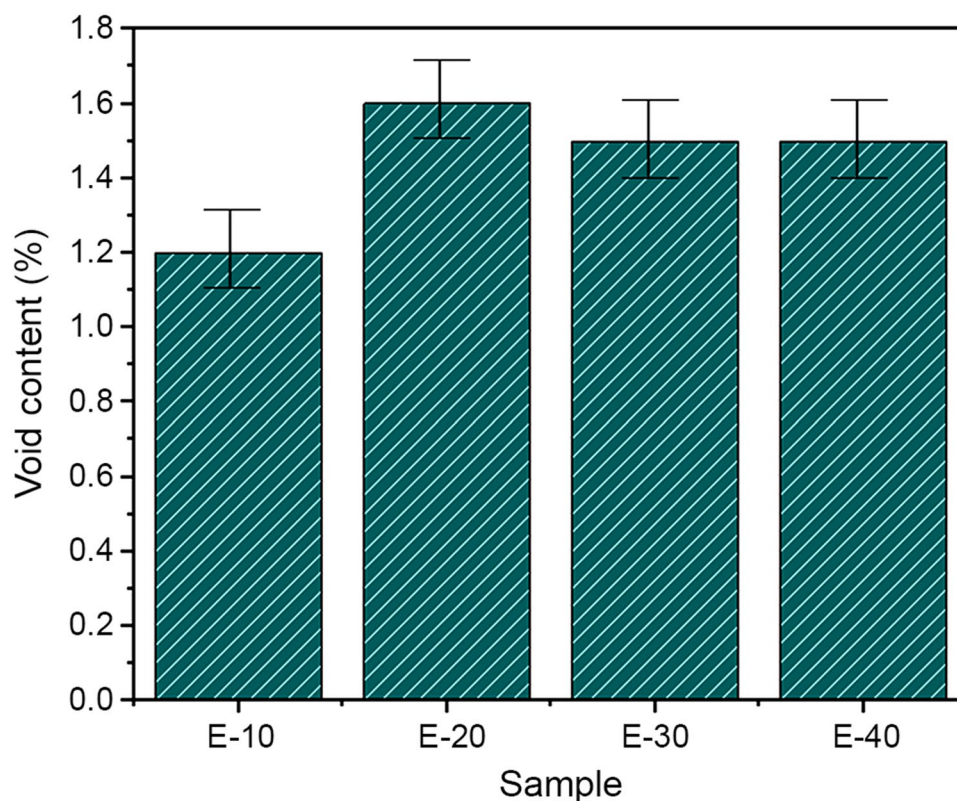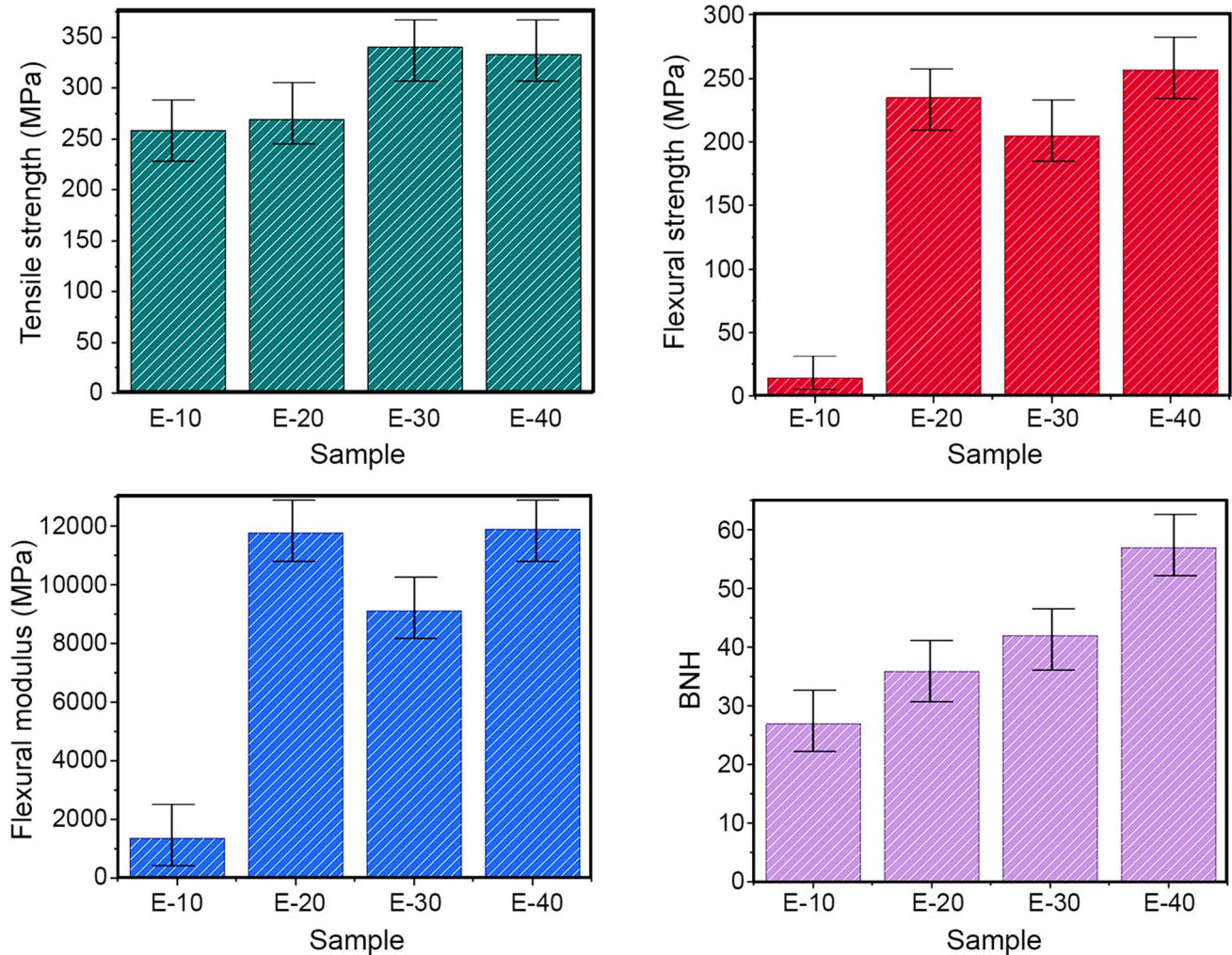
Fig. 3 Tensile strength **a** flexural strength **b** modulus **c** and hardness **d** versus types of composite samples

in this research work. Understandably, the highest value of tensile strength, flexural modulus, and flexural strength was achieved for the composites with 5 and 10% (by wt) of α-Al$_2$O$_3$ NPs, respectively. As can be seen in Fig. 3a, the highest tensile strength in this study belongs to the E-30 sample which was increased from 259 MPa (sample E-10 was selected as highest mechanical performance in prototype) to 341 MPa and shows 24% enhancement compared to other samples. In the flexural test (Fig. 3b and c), the maximum improvement for flexural strength (95.5%) was related to the E-40 sample; indeed for this content of α-Al$_2$O$_3$ NPs, flexural modulus demonstrates the highest value with 91.8% enhancement. Since E-10 or the prototype was not modified with NPs, it showed lower mechanical properties than modified samples. For example, it was evident that the samples having NPs showed higher mechanical properties after the addition of NPs. Another effective parameter that played a major role in

mechanical properties was the adhesion between the reinforcements and matrix. In these samples, the adhesion between matrix and reinforcements led to the transmission of the applied forces and stresses from the matrix to the reinforcements. NPs can improve and increase the bonds between the fibers and the resin, which in turn increase the strength of the composite structure and improve the adhesion property. Therefore, the improvement of tensile properties and flexural properties was related to the presence of α-Al$_2$O$_3$ NPs within the carbon fiber/epoxy resin which led to an enhancement in interfacial strength. Additionally, when the crack started to grow the nanoparticles prevented their growth or created another path. This factor has prevented the sudden and global failure of the sample [48]. The obtained results are in good agreement with previous studies [49]. The summation of the obtained results from the mechanical investigation displays that the better result is related to composites having α-Al$_2$O$_3$ NPs.

Hardness assessment

Figure 3d shows BNH versus an increase in the percentage of the used α-Al_2O_3 NPs in the hybrid composite. The sample showing maximum BHN displays superior hardness. The findings illustrated that the hybrid composite structure, reinforced by 10% α-Al_2O_3 NPs, displayed maximum hardness that may be related to their homogenous distribution in the composite structure and lower interparticle space by increasing the NPs loading in the polymeric matrix. By considering the achieved effects, it is detected that an increase in the accumulation of α-Al_2O_3 NPs enhanced the hardness of the composite structure. This performance is due to stronger bonding between the reinforcement and modified matrix.

Morphological analysis

The morphology of α-Al_2O_3 NPs, used in the preparation of the composite, is displayed in Fig. 4. NPs incline to form agglomerates because of several forces. Therefore, it is predictable that the agglomeration of NPs can create numerous stress and flaws in the structures of the hybrid composite [50]. Aluminum oxide NPs generally accumulate after the ultrasonic process, and the dispersion distribution is not well done. The sonication of NPs by section solution in the matrix is a useful way that could prevent their agglomeration even at high NPs concentrations.

FE-SEM analysis was used to study the morphology of the samples after undergoing mechanical tests. Figure 5a-b displays the effect of mechanical study on the structure of the fabricated composites. As a result of the unfortunate interlaminar interfaces, extra delamination and structural damages are detected in CF/unmodified epoxy composite structure (Fig. 5a) in compared to 10% (by wt) α-Al_2O_3 NPs-modified resin (Fig. 5c). These FE-SEM images show that interlaminar connection is significantly enhanced through the modified epoxy resin. As perceived in Fig. 5a-b, CF pull-out [51] and CF breakage [52], which are a sign of weak adhesion of CF/epoxy, occur within unmodified hybrid composite structures. In contrast, when the polymeric resin was adapted (10% (by wt) α-Al_2O_3 NPs), fiber breakage and fiber pull-out trends have not been strictly detected. Alternatively, a perfect sign of improved CF/epoxy boundary adhesion through the

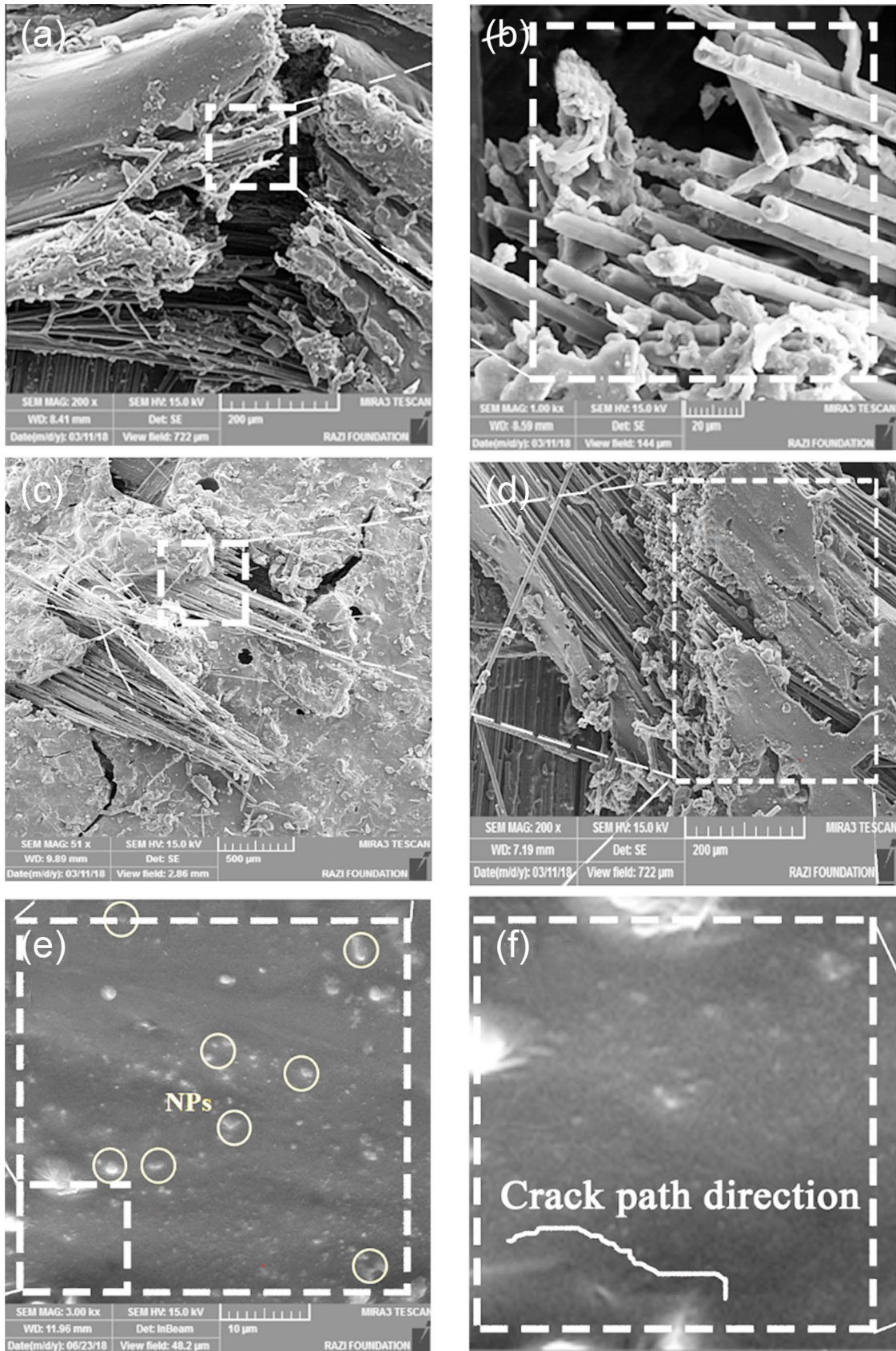**Fig. 4** FE-SEM image of α-Al_2O_3 NPs
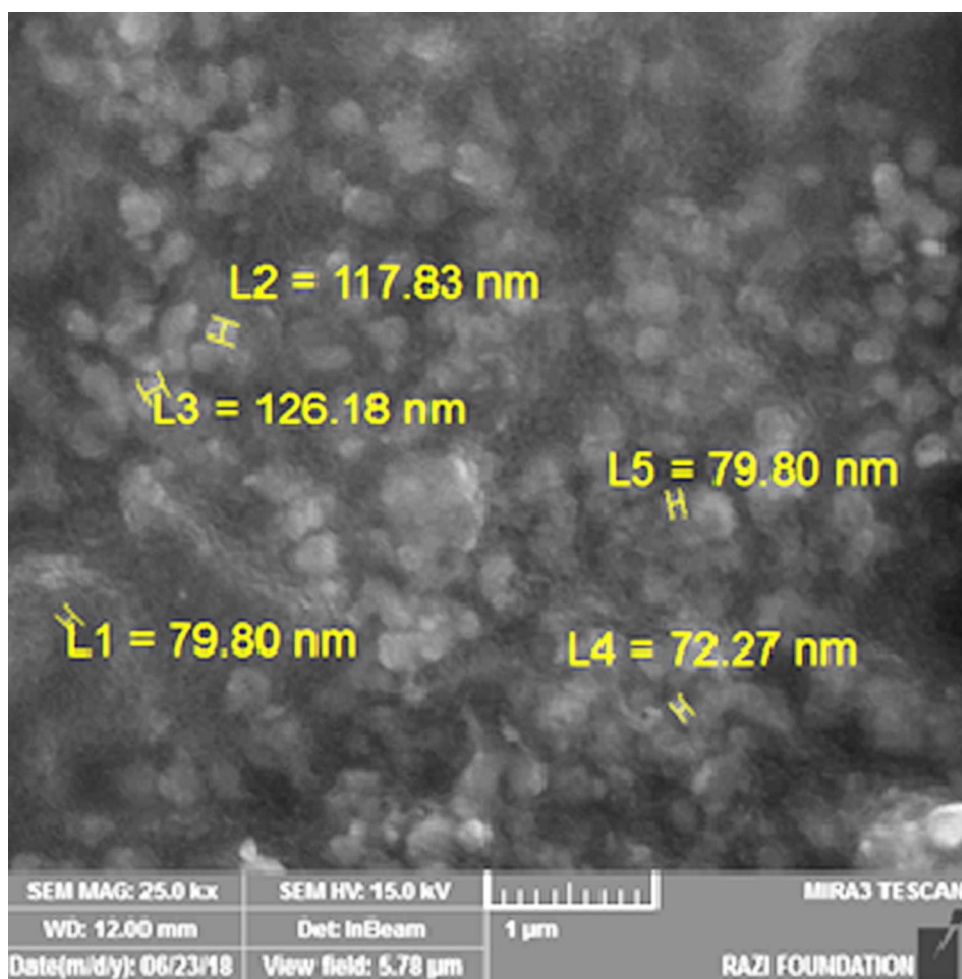
Fig. 5 FE-SEM images of CF/epoxy composite structures: **a**-**b** for unmodified epoxy/CF and **c**–**f** for 10 wt% α-Al$_2$O$_3$ NPs-CF/epoxy

resin rupture characteristics on pull-out CF is perceived in Fig. 5d. Besides, it is observed in Fig. 5c–d that hardening mechanisms for instance crack path deflection occurs after the polymeric resin is improved by 10% (by wt) α-Al$_2$O$_3$ NPs.

FE-SEM images of the systems with different ratios of α-Al$_2$O$_3$ NPs (2, 5, and 10% by wt) are exhibited in Fig. 5e–f. From Fig. 5e, it is seen that the α-Al$_2$O$_3$ NPs were distributed homogeneously in the structure of the composites. As can be seen in the microscopic image, the NPs have no aggregation and the dispersion is well distributed and dispersed in the sample. It is anticipated that the uniform dispersion of α-Al$_2$O$_3$ NPs in the structure of the composites could have a positive influence on their mechanical properties. As it is evident, small round-shaped α-Al$_2$O$_3$ NPs with an average diameter of 90 nm were uniformly dispersed in the hybrid composite. As it is shown, the distribution of NPs in the samples is noticed in Fig. 6. Figure 6a shows a sample without NPs, while Fig. 6b–d shows samples with percentages of 2.5 and 10%, respectively. EDS analysis of the E-40 composite as a model of the fabricated samples is shown in Fig. 6e. EDS analysis displayed the presence of only C, O, and

Al elements in the structure of E-40 and is a sign that the composite structure comprises NPs reinforcement.

Thermal study

The TGA analysis was used to study the thermal behavior of the prepared hybrid composites. The obtained TGA and DTA results for the hybrid composites are illustrated in Fig. 7. As it is shown in this figure, for E-10 a major destruction has occurred between 420 °C and 521 °C (45%) which is due to the destruction and evaporation of epoxy resin and carbon fiber present in the hybrid composites. For E-20 sample, the solvent removal was carried out at 100 °C. Major destruction of this sample started at 291 °C, and the weight loss stage was continued until 643 °C. The observed major weight loss (44%) was due to the volatilization and degradation of epoxy resin and carbon fiber. E-30 sample showed an initial degradation at 98 °C, which was due to the solvent removal from the hybrid composite. For this sample, the major destruction (60%) started at 299 °C and continued until 591 °C which was because of the volatilization and degradation of epoxy resin and carbon fiber. The TGA of E-40 demonstrated the initial weight loss at 98 °C, while the major weight loss
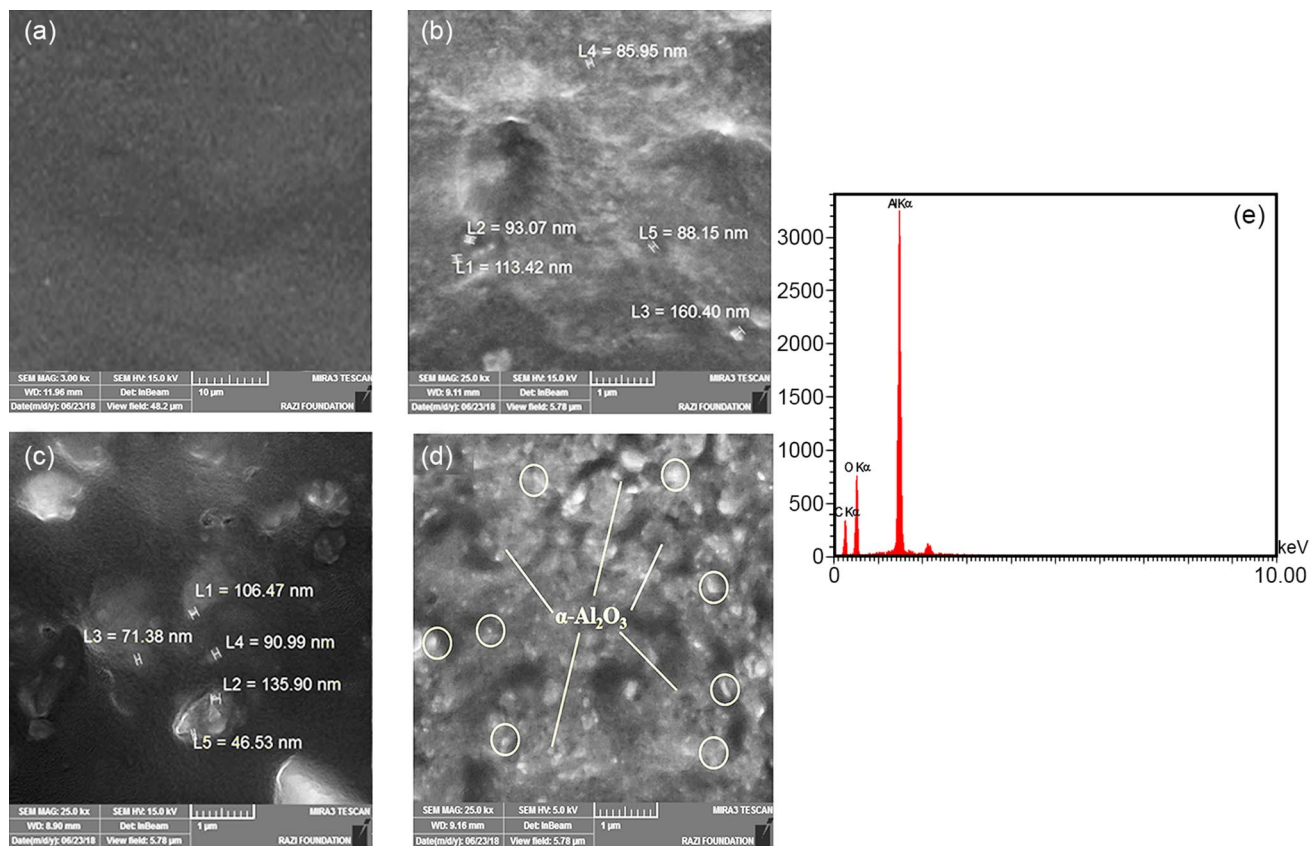

Fig. 6 FE-SEM images: E-10 sample **a** E-20 sample **b** E-30 sample **c** E-40 sample **d** and EDS of E-40 sample **e**
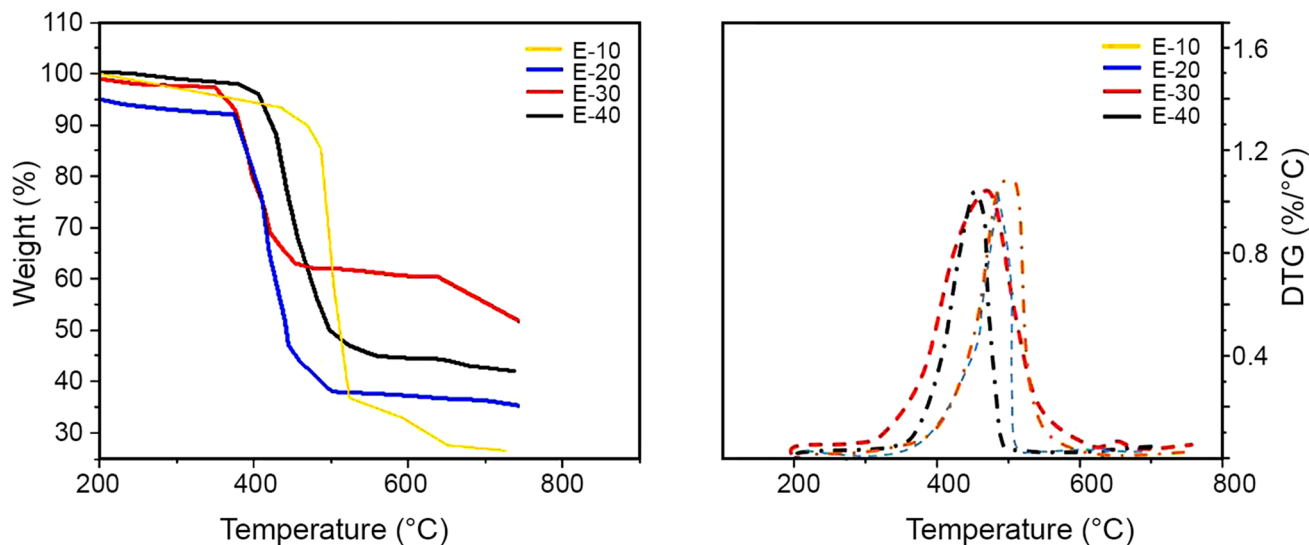
Fig. 7 TGA curves and DTG of the prepared composite samples

(62.5%) was started at 379 °C and continued till 559 °C which was due to the volatilization and degradation of epoxy resin and carbon fiber [53]. The TGA analysis showed that by the selection of a specific percentage of α-Al_2O_3 NPs we can acquire a composite with desired thermal stability [54, 55].

Conclusion

The present paper reports the effect of α-Al_2O_3 NPs on the thermal and mechanical properties of the carbon fiber/epoxy resin hybrid composites. Major achievements of the current study are listed as follows: uniform distribution of α-Al_2O_3 NPs in the carbon fiber/epoxy resin hybrid composites led to an impressive improvement on the flexural strength, tensile strength, flexural modulus, and hardness. Variations in the properties of the composite by addition of NPs due to the good adhesion between the resin and the fibers. The thermal stability is decreased in hybrid composites by α-Al_2O_3 NPs loading which shows the effect of composite components on the final properties. The conclusion of this study revealed that modified epoxy resin (with 10% by wt of α-Al_2O_3 NPs) could be a prospective candidate as operational materials under dissimilar load owing to its enhanced properties. Based on the obtained results, the prepared hybrid composite potentially could be used in industry due to its good mechanical properties.

Declarations

Conflict of interest The authors declare that there is not any conflict of interest.

References

1. Chowdhury P, Sehitoglu H, Rateick R (2018) Damage tolerance of carbon-carbon composites in aerospace application. Carbon 126:382–393
2. Tekin E, Kapan Ö (2016) Composite manufacturing data management in aerospace industry. Procedia CIRP 41:1039–1042
3. Hou P, Li R, Li Q, Lu N, Wang K, Liu M, Cheng X, Shah S (2018) Novel superhydrophobic cement-based materials achieved by construction of hierarchical surface structure with FAS/SiO_2 hybrid nanocomposites. ES Mater Manuf 1:57–66
4. Naskar AK, Keum JK, Boeman RG (2016) Polymer matrix nanocomposites for automotive structural components. Nat Nanotechnol 11:1026–1030
5. Balakrishnan VS, Seidlitz H (2018) Potential repair techniques for automotive composites: a review. Compos Part B: Eng 145:28–38
6. Deshmukh K, Ahamed MB, Sadasivuni KK, Ponnamma D, Deshmukh RR, Trimukhe AM, Pasha SKK, Polu AR, AlMaadeed MA-A, Chidambaram K (2017) Solution-processed white graphene-reinforced ferroelectric polymer nanocomposites with improved thermal conductivity and dielectric properties for electronic encapsulation. J Polym Res 24
7. Alsaadi M, Bulut M, Erkliğ A, Jabbar A (2018) Nano-silica inclusion effects on mechanical and dynamic behavior of fiber reinforced carbon/Kevlar with epoxy resin hybrid composites. Compos Part B Eng 152:169–179
8. An Q, Chen J, Ming W, Chen M (2020) Machining of SiC ceramic matrix composites: a review. In press, Chin J Aeronautics
9. Yıldız H, Tokalıoğlu Ş, Soykan C (2021) Preparation of polyacrylonitrile/polyindole conducting polymer composite and its use for solid phase extraction of copper in a certified reference material. Spectrochim Acta Part A Mol Biomol Spectr 244:118826

10. Manivannan I, Ranganathan S, Gopalakannan S (2019) Tribological behavior of aluminum nanocomposites studied by application of response surface methodology. Adv Compos Hybrid Mater 2:777–789

11. Ma Y, Zhuang Z, Ma M, Yang Y, Li W, lin J, Dong M, Wu S, Ding T, Guo Z, (2019) Solid polyaniline dendrites consisting of high aspect ratio branches self-assembled using sodium lauryl sulfonate as soft templates: synthesis and electrochemical performance. Polymer 182:121808

12. Ma Y, Ma M, Yin X, Shao Q, Lu N, Feng Y, Lu Y, Wujcik EK, Mai X, Wang C, Guo Z (2018) Tuning polyaniline nanostructures via end group substitutions and their morphology dependent electrochemical performances. Polymer 156:128–135

13. Tabrizi AG, Arsalani N, Namazi H, Ahadzadeh I (2017) Vanadium oxide assisted synthesis of polyaniline nanoarrays on graphene oxide sheets and its application in supercapacitors. J Electroanal Chem 798:34–41

14. Tabrizi AG, Arsalani N, Mohammadi A, Namazi H, Ghadimi LS, Ahadzadeh I (2017) Facile synthesis of a $MnFe_2O_4/rGO$ nanocomposite for an ultra-stable symmetric supercapacitor. New J Chem 41:4974–4984

15. Namazi H, Belali S (2016) Starch-g-lactic acid/montmorillonite nanocomposite: synthesis, characterization and controlled drug release study. Starch-Stärke 68:177–187

16. Nia SB, Pooresmaeil M, Namazi H (2020) Carboxymethylcellulose/layered double hydroxides bio-nanocomposite hydrogel: a controlled amoxicillin nanocarrier for colonic bacterial infections treatment. Int J Biolog Macromol 155:1401–1409

17. Pooresmaeil M, Namazi H (2018) Surface modification of graphene oxide with stimuli-responsive polymer brush containing β-cyclodextrin as a pendant group: preparation, characterization, and evaluation as controlled drug delivery agent. Colloid Surf B: Biointerf 172:17–25

18. Namazi H, Fard AMP, Pooresmaeil M (2019) Peripherally functionalized based dendrimers as the template for synthesis of silver nanoparticles and investigation the affecting factors on their properties. Polym Bull 76:4659–4675

19. Kretsis G (1987) A review of the tensile, compressive, flexural and shear properties of hybrid fibre-reinforced plastics. Composites 18:13–23

20. Li S, Lin Q, Zhu H, Cui C, Hou H, Lv T, Li Y (2016) Investigations on mechanical characteristics of glass fiber reinforced epoxy composite modified with amino-terminated hyperbranched polymer. Fiber Polym 17:282–288

21. Mechtcherine V, Michel A, Liebscher M, Schneider K, Großmann C (2020) Mineral-impregnated carbon fiber composites as novel reinforcement for concrete construction: material and automation perspectives. Auto Constr 110:103002

22. Neto DBF, Xavier FFS, Matsubara EY, Parmar R, Gunnella R, Rosolen JM (2020) The role of nanoparticle concentration and CNT coating in high-performance polymer-free micro/nanostructured carbon nanotube-nanoparticle composite electrode for Li intercalation. J Electroanal Chem 858:113826

23. Makeev A, Ghaffari S, Seon G (2019) Improving compressive strength of high modulus carbon-fiber reinforced polymeric composites through fiber hybridization. Int J Eng Sci 142:145–157

24. Zhao X, Chen H, Wang S, Wu Q, Xia N, Kong F (2018) Electroless decoration of cellulose paper with nickel nanoparticles: a hybrid carbon fiber for supercapacitors. Mater Chem Phys 215:157–162

25. Bustero I, Gaztelumendi I, Obieta I, Mendizabal MA, Zurutuza A, Ortega A, Alonso B (2020) Free-standing graphene films embedded in epoxy resin with enhanced thermal properties. Adv Compos Hybrid Mater 3:31–40

26. Zhang X, Chen Z, Li K, Yang Z, Li Z, Xie D, Zhou W, Wang T, Ma S, Burns R, Ruso JM, Tang Z, Liu Z (2019) Immobilization of penicillin G acylase on a novel paramagnetic composite carrier with epoxy groups. Adv Compos Hybrid Mater 2:720–734

27. Namazi H, Ahmadi H (2011) Improving the proton conductivity and water uptake of polybenzimidazole-based proton exchange nanocomposite membranes with TiO_2 and SiO_2 nanoparticles chemically modified surfaces. J Power Sourc 196:2573–2583

28. Zhang D, Sun J, Lee LJ, Castro JM (2020) Overview of ultrasonic assisted manufacturing multifunctional carbon nanotube nanopaper based polymer nanocomposites. Eng Sci 10:35–50

29. Yan X, Liu J, Khan MA, Sheriff S, Vupputuri S, Das R, Sun L, Young DP, Guo Z (2020) Efficient solvent-free microwave irradiation synthesis of highly conductive polypropylene nanocomposites with lowly loaded carbon nanotubes. ES Mater Manuf 9:21–33

30. Pooresmaeil M, Namazi H (2019) Preparation and characterization of polyvinyl alcohol/β-cyclodextrin/GO-Ag nanocomposite with improved antibacterial and strength properties. Polym Adv Technol 30:447–456

31. Mahato KK, Dutta K, Ray BC (2019) Assessment of mechanical, thermal and morphological behavior of nano-Al_2O_3 embedded glass fiber/epoxy composites at in-situ elevated temperatures. Compos Part B: Eng 166:688–700

32. Wang C, Zhao M, Li J, Yu J, Sun S, Ge S, Guo X, Xie F, Jiang B, Wujcik EK (2017) Silver nanoparticles/graphene oxide decorated carbon fiber synergistic reinforcement in epoxy-based composites. Polymer 131:263–271

33. Sonmez M, Ficai D, Ardelean IL, Trusca R, Alexandrescu L, Constantinescu D, Ghizdavet Z, Oprea O, Ficai A, Andronescu E (2019) Flax fibres fabric surface decoration with nanoparticles-a promising tool for developing hybrid reinforcing agent of thermoplastic polymers. Fiber Polym 20:2407–2415

34. Taketa I, Ustarroz J, Gorbatikh L, Lomov SV, Verpoest I (2010) Interply hybrid composites with carbon fiber reinforced polypropylene and self-reinforced polypropylene. Compos Part A Appl Sci Manuf 41:927–932

35. Atiqah A, Maleque M, Jawaid M, Iqbal M (2014) Development of kenaf-glass reinforced unsaturated polyester hybrid composite for structural applications. Compos Part B Eng 56:68–73

36. Sun L, Liang L, Shi Z, Wang H, Xie P, Dastan D, Sun K, Fan R (2020) Optimizing strategy for the dielectric performance of topological-structured polymer nanocomposites by rationally tailoring the spatial distribution of nanofillers. Eng Sci 12:95–105

37. Dong C, Davies IJ (2014) Flexural and tensile strengths of unidirectional hybrid epoxy composites reinforced by S-2 glass and T700S carbon fibres. Mater Des 1980–2015(54):955–966

38. Dong C, Davies IJ (2014) Flexural and tensile moduli of unidirectional hybrid epoxy composites reinforced by S-2 glass and T700S carbon fibres. Mater Des 1980–2015(54):893–899

39. Li J, Xia YC (2009) The reinforcement effect of carbon fiber on the friction and wear properties of carbon fiber reinforced PA6 composites. Fiber Polym 10:519–525

40. Xie P, Zhu S, Shao Y, Peng W, Zhan L, Li S (2019) Simulation and experimental analysis of autoclave co-curing CFRP hat-stiffened panels with silicone airbag mandrels. Iran Polym J 28:505–514

41. Ipakchi H, Shegeft A, Rezadoust AM, Zohuriaan-Mehr MJ, Kabiri K, Sajjadi S (2020) Bio-resourced furan resin as a sustainable alternative to petroleum-based phenolic resin for making GFR polymer composites. Iran Polym J 29:287–299

42. Sørensen BF, Goutianos S (2018) Increase of fracture resistance by the interaction of two cracks-cohesive law scale effects. In: 7th Eur Conf Comput Fluid Dynamics (ECFD 7)

43. Piao H, Kiryu Y, Chen L, Yamashita S, Ohsawa I, Takahashi J (2019) Influence of water absorption on the mechanical properties of discontinuous carbon fiber reinforced polyamide 6. J Polym Res 26:1–8

44. Xiong C, Li Q, Lan T, Li H, Long W, Xing F (2021) Sustainable use of recycled carbon fiber reinforced polymer and crumb rubber in concrete: mechanical properties and ecological evaluation. J Clean Prod 279:123624

45. Shi L, Song G, Li P, Li X, Pan D, Huang Y, Ma L, Guo Z (2021) Enhancing interfacial performance of epoxy resin composites via in-situ nucleophilic addition polymerization modification of carbon fibers with hyperbranched polyimidazole. Compos Sci Technol 201:108522

46. Shi K, Shen Y, Zhang Y, Wang T (2018) A modified imidazole as a novel latent curing agent with toughening effect for epoxy. Eng Sci 5:66–72

47. ASTMCASTM Standards 1958 In: American Society for Testing Materials Philadelphia

48. Eskizeybek V, Ulus H, Kaybal HB, Şahin ÖS, Avcı A (2018) Static and dynamic mechanical responses of CaCO$_3$ nanoparticle modified epoxy/carbon fiber nanocomposites. Compos Part B Eng 140:223–231

49. Alsaadi M, Erkliğ A (2018) Effect of perlite particle contents on delamination toughness of S-glass fiber reinforced epoxy matrix composites. Compos Part B Eng 141:182–190

50. Zare Y (2016) Study of nanoparticles aggregation/agglomeration in polymer particulate nanocomposites by mechanical properties. Compos Part A Appl Sci Manuf 84:158–164

51. Kagitci YC, Tarakcioglu N (2016) The effect of weld line on tensile strength in a polymer composite part. Int J Adv Manuf Technol 85:1125–1135

52. Cheng X, Du X, Zhang J, Zhang J, Guo X, Bao J (2018) Effects of stacking sequence and rotation angle of patch on low velocity impact performance of scarf repaired laminates. Compos Part B Eng 133:78–85

53. Jing X, Wei J, Liu Y, Song B, Liu Y (2020) Deployment analysis of aramid fiber reinforced shape-memory epoxy resin composites. Eng Sci 11:44–53

54. Wei W, Qi X, Li J, Zhong Y, Zuo G, Pan X, Su T, Zhang J, Dong W (2017) Synthesis and characterization of a novel cationic hydrogel base on salecan-g-PMAPTAC. Int J Biolog Macromol 101:474–480

55. Qi X, Wei W, Li J, Zuo G, Hu X, Zhang J, Dong W (2016) Development of novel hydrogels based on Salecan and poly(N-isopropylacrylamide-co-methacrylic acid) for controlled doxorubicin release. RSC Adv 6:69869–69881